Calibration of the 1.0 x 0.7m Low Speed Wind Tunnel of Tottori University

By

Fumio YOSHINO and Shinichi MORI

(Received September 8,)

Summary

The calibration of the tunnel had been carried out in about six months from September, 1969 through February, 1970.

The calibration was made on velocity distributions, static pressure distributions along and perpendicular to the tunnel axis, angular variation of flow and drag coefficient of two dimensional circular cylinders. The results are given in Figs. 4 to 9. Though there still remains surging at a rate of fluctuation of 1mmAq per dynamic pressure of 170mmAq in the test section, the tunnel has satisfactory performance characteristics as a low speed tunnel.

I Introduction

1.1 *INTRODUCTION*-The tunnel had been designed by us, constructed by the employee of the university in about nine months and completed by the end of March, 1969.

The tunnel was designed to give continuously variable tunnel speed from 15m/s to 45m/s so as to be capable of carrying out both experiments of turbulent boundary layer and a small model with dimensions of 100mm chord and 6.7 of aspect ratio at the Reynolds number higher than 3×10^5 when the tunnel is run at higher speed.

The type of the tunnel, Goettingen type with a closed test section, was chosen from the view point of getting lower turbulence and higher velocity at the test section with less power requirement.

The tunnel (Fig. 1) had strong surging of order of fluctuation of about 50mm Aq per dynamic pressure of 130mmAq in the test section. After the fan test, the performance curves of the fan were found to show no pulsation point, that is, static pressure monotonously decreases as flow rate increases. The surging was found associated with the diffuser after the test section and the corner right behind it. Therefore the inlet of the diffuser was reshaped to one as shown in Fig. 2 and four guide vanes were fixed along stream lines of potential flow in the diffuser. In addition to these, the most inside corner vane was extended by 250mm downstream. After such improvement, the surging was reduced to the fluctuation of 1mmAq per dynamic pressure of 170mmAq in the test section. Such a small fluctuation does not cause considerable changes in the aerodynamic characteristics of test model[1),2),3)]. Therefore the calibration was made under this condition.

The maximum tunnel speeds measured are 54m/s for the closed diffuser (Fig. 1) and 52m/s for the improved diffuser (Fig. 2) . In practice the tunnel speed can be continuously changed from 0 to the maximum speed though the driving motor is designed to change RPM from 500 to 1500.

1.2 *RANGE OF INVESTIGATION*-[2),4)]. complete traverses across the test section were made in two planes at 55mm (name this an inlet-plane) and 1410mm (an outlet-plane) from the inlet of the test section.

Measurements in each plane at 100mm intervals vertically (row) and horizontally (line) . Each row has 7 points and each line 9 points. Each row is named the rows 1, 2, 3, … and so on from port to starboard and each line the lines a, b, c, … and the like from up to down. In addition to these velocity measurements at 63 points in a plane, velocity profiles of boundary layer of the floor and the ceiling were determined in the inlet-plane and the outlet-plane.

The tests were designed to give the following informations:

(1) Velocity distribution contours over the inlet-plane and outlet-plane at tunnel speeds of 20m/s and 52m/s.

(2) Thickness of boundary layer at the inlet-and outlet-planes.

(3) Static pressure over the same planes as in (1) and along the tunnel axis at the same speeds.

(4) Drag coefficient of two dimensional circular cylinders and a disc.

In addition to these, angular flow variations were checked at three points on a horizontal line through the center of the cross section at 720mm from the inlet of the test section.

The details of the experimental procedure are given in an Appendix.

II Results

2.1 *VELOCITY DISTRIBUTION*- Velocity distribution contours at 52m/s over the inlet- and outlet- planes are shown in Figs. 4 and 5 respectivly.

These curves are drawn so that the observer faces upstream into the nozzle. The curves in the figures indicate that velocity on a curve is higher by the proportion designated than velocity at the center of the plane. C in the figures is a square root of $q/\Delta p$, ratio of dynamic pressure q measured at a point to static pressure difference Δp between static pressure near the inlet of the test section and that near the inlet of the nozzle. Co is C at the center of the plane.

The maximum local velocity in the inlet-plane exists in the right corner near the floor. It is approximately 1.7% faster than that at the center. In general, velocity is faster near the four corners and slower near the center. However variation of local velocity from the mean is within ± 0.3% for the most part of the inlet-plane.

Variation of local velocity is considerably larger in the outlet-plane than in the inlet-plane as shown in Fig. 5.

The general tendency is similar to that in the inlet-plane. In this case, the variation from the mean is less than ± 1% in a good part of the outlet-plane. Lower velocity near the center of the planes seems to be caused due to the hub of the fan and 220 mesh screen of 0.5mm diameter wire put across the inlet of the central diffuser formed by the guide vanes (Fig. 2) . Effect of the screen on the velocity distribution is reasonably stronger in the outlet-plane than in the inletplane, which gives more variation from the mean in the former.

At the tunnel speed of 20m/s, which is not shown here, the maximum deviation of the velocity from the mean is about ± 3.5% in the inlet-plane and ± 5% in the outlet-plane. The points of larger deviation occur near the floor and the ceiling. Inside the rectangle constructed by the lines a, b, and rows 1 and 9, the variation from the mean is less than ± 3.0% in both of the inlet and outlet-planes.

Certainly, velocity distribution becomes worse at lower velocity.

2.2 *THICKNESS OF BOUNDARY LAYER*- Fig. 6 shows the velocity profiles inside and outside of boundary layers at rows 3, 5, and 7 in the inlet-plane at tunnel speed of 52m/s.

Thickness of boundary layer is approximately 15mm on both of the floor and the ceiling. It must be mentioned that the unit of the ordinate, Z is enlarged near the floor and the ceiling.

In the outlet-plane (not shown here) , thickness varies from 25mm to 35mm depending on the point of measurement. This discrepancy seems to take place due to the unevenness of the surface and the tape sticked to cover holes in the floor and the ceiling.

At lower speed (20 m/s) , thickness is less than 10mm in the inlet-plane and 15mm to 30mm in the outlet-plane.

2.3 *STATIC PRESSURE AND ANGULAR FLOW VARIATION*-Static pressure across the plane (at 52m/s) is shown in Fig. 7 as a fraction of dynamic pressure. Static pressure near the floor and the ceiling is lower in comparison with that on the horizontal line through the center of the plane, which coincides with the fact that velocity is faster near both surfaces. Irregularity at row 7 in the inlet-plane is due to the unevenness of the surfaces of the test section and the nozzle, which is also in accordance with the velocity distribution in the inlet-plane (Fig. 4) . The maximum variations from the mean of p_s/q are ± 0.029 in the inlet-plane and ± 0.042 in the outlet-plane.

Static pressure at tunnel speed of 20m/s (not shown here) is at the maximum variation of ± 0.036 and ± 0.039 from the mean in the inlet-and the outlet-planes respectively. By and large static pressure distributions at lower speed and higher speed are much alike but it is worse at lower speed than at higher speed as in case of velocity distribution.

Static pressure along the tunnel center line is shown in Fig. 8 as a fraction of dynamic pressure. It is seen that static pressure falls by degrees along the tunnel axis up to 500mm from the inlet of the test section, is nearly constant over a considerable portion of the test section (up to 1000mm) and rises again on approaching the outlet. This rise near the outlet is caused due to the screen put across the inlet of the diffuser and is in accordance with worse velocity distribution there.

Longitudinal buoyancy is of order of 13 gr at 52m/s for a circular cylinder of 500mm long and 100mm in diameter mounted parallely to stream on the balance.

Angular flow variations at 52m/s are 0.7 degrees more downwards and 0.3 degrees more rightwards at point A compared with that at point C. (See Appendix) . It is about the same at 20 m/s too within experimental error. However these values imply only relative directions of wind at point A to that at point C. It is necessary to make use of more sophisticated apparatus for the measurement of angular variation relative to the tunnel axis.

2.4 *DRAG COEFFICIENT* - Drag coefficients of two dimensional cylinders and a circular disc are plotted in Fig. 9 in which a solid line is a result in Goettingen.[5] Drag coefficient of cylinders shows that transition from laminar to turbulent flow occurs at $Re = 4 \times 10^5$.

Higher C_D (=0.4) at the transition point seems due to surface roughness[6] of a cylinder made of hard vinyl resin, while there being no such scratches on the surface of the other two steel cylinders. Drag coefficient of a circular disc is independent of Reynolds number in the range of the experiment and is equal to 1.18 on an average.

Ⅲ Concluding Remarks

(1) The tunnel is satisfactory in velocity uniformity over the inlet- and outlet-planes, longitudinal static pressure distribution and the magnitude of turbulence.

(2) Surging still remains at the proportion of fluctuation of 0.6% per dynamic pressure of 170mmAq. It is expected to be cured when the inside surfaces of the diffuser and corner will be carefully faired or a small portion of air is to be sucked out.

References

(1) Golin, S. M. and Slezinger, I. I., "Wind tunnels and their instrumentation", Chap. 2, (1966) Israel Program For Scientific Translation, Jerusalem.

(2) Pope, A., "Wind-tunnel testing", Chap. 3, (1964) John Wiley & Sons, New York.

(3) Pankhurst, R. C. and Holder, D. W., "Wind-tunnel technique", Chap. 2, (1968) Sir Isaac Pitman & Sons, London.

(4) Allen, J. E. and Diprose, K. V., R. & M. 2566 (1942)

(5) Japan Aeronautics Conference, "Wind tunnel testing directory", 56 (1943) Japan Aeronautics Conference. (Kōkū-hyōgikai, "Fūdō Shiken Kitei", 56 (1943) Kōkū-hyōgikai.)

(6) Goldstein, S., "Modern developments in fluid dynamics", Chap. 9, (1965) Dover, New York.

Appendix

(1) *TUNNEL* - The plan view of the tunnel is shown in Fig. 1. The total length, width and height are 12460mm, 5800mm and 2950mm respectively. The height of the test section is 1925mm from the ground level. The part of the test section is in a building and the part of return flow outside.

The axial flow fan made by Nakanishi Kinzoku Kogyo K. K. has the dimension of 1650mm in diameter and 3325mm long and is designed to give flow rate of $1890m^3$/min and 85mmAq static pressure rise at the running speed of 900 rpm.

It is driven through pulleys and V belts by means of KS, 53/22p Motor which is a product of Fuji Electric Co.,Ltd. and has torque of 32.4 kg-m at 1500 rpm and the speed of which is continuously variable from 500 to 1500 rpm.

The diffuser after the fan is 4300mm in length, 1650mm and 2050mm in width at the inlet of and the outlet of the diffuser respectively.

The corner vanes are steel plates 2.3mm thick bent along a circular arc. The mean cell width of the honeycomb is 2% of width of the settling chamber, thickness of the honeycomb being 5 times the mean cell width. There are three screens after the honeycomb, the first of which is a 17 mesh screen with 2mm diameter wire, the secnd a 66 mesh screen with 1.0mm diameter wire, the third a 220 mesh screen with 0.5mm diameter wire.

The nozzle profile is similar to Vitoshinskii curve[1)] and has a contraction ratio of 6.

The test section consists of aluminum alloy plate 10mm thick (floor) , steel plates 2.3mm thick (ceiling and wall) and transparent acrylic resin plate 10mm thick (wall) , the dimension of that being 1000mm wide, 700mm high and 1500mm long.

The diffuser after improvement is shown in Fig. 2.

The tunnel is welded from steel plates 4.5mm thick and 6.0mm thick. The inside is painted with anticorrosive paint.

(2) *APPARATUS AND METHOD OF MEASUREMENT* - Tunnel speed is controlled by varying static pressure difference, Δp mmAq which is the difference between static pressures near the test section inlet and the nozzle inlet, Δp is of course

linearly dependent on dynamic pressure in the test section, from which velocity in the test section is deduced. The relationship of Δp to dynamic pressure is determined by making use of a pitot-static tube of 6mm in diameter and a shank 380mm long of Rikaseiki Kogyo K. K. which is also used to determine the static pressure along the tunnel axis. Pressures of all kind were observed by means of Goettingen manometers of 300mm high.

The empirical formula of the relation is $q_m = 1.056 \times \Delta p$ (mmAq) where q_m is mean dynamic pressure in the inlet-plane outside boundary layer.

Velocity and static pressure distributions are determined by a pitot-static tube of 12mm in diameter and shank 1000mm long with wooden tail fairing of Rikaseiki Kogyo K. K. The tube was slided along steel angle perpendicular to flow direction that is firmly fixed on to the test section.

Measurement of static pressure at 10 points along the flow-direction is made in fact along the line shifted by 50mm to the port from the center line.

A spherical pitot tude of 6mm in diameter with 5 holes on it (F200 of Rikaseiki Kogyo K. K.) was made use of to determine angular variation of flow. The pitot tube was fixed on the stand which would be slided on steel angle perpendicular to flow direction. The contact surfaces of them were finished with a scraper. Maximum angular variaton of the yaw head when slided along the angle was less than 10 minutes when measured in the shop. However, the yaw head was neither aligned to the direction of the tunnel axis nor calibrated.

Therefore, we could only determine the relative angular variation of flow between points A, B and C.

These three points A, B and C are horizontally positioned at 292mm port of the tunnel axis, tunnel axis and 301mm starboard of the axis respectively in the cross section at 750mm from the inlet of the test section.

Measurement of boundary layer was made with a total head tube with a branch of 1.55mm in diameter and a shank 1000mm long to have steel tail fairing.

It was measured at rows, 1, 2,…8 and 9 in the inlet - and outlet-planes. Static pressures at lines a and g were made use of when velocity in boundary layer was deduced from the observation.

Drag coefficient was determined on three two dimensional circular cylinders. A 160mm cylinder is of 162.27mm in diameter and 509mm long, a 32mm cylinder of 32.7mm in diameter and 500mm long and a 10mm cylinder of 10.13mm in diameter and 500mm long. Though they were carefully finished with powder of aluminum oxide, a 160mm cylinder had small scratches on it while the other two did not since the former was a vinyl resin pipe and the latters were steel pipes. These were mounted on a three components balance, a product of Sonoike Tool Manufasturing Co., LTD. having the range of measurement of lift force, drag force and pitching moment less than 50kg, 10kg, and ± 5kgm respectively.

The skelton of the balance is shown in Fig. 3. Two dummies for each cylinder were aligned to the latter and firmly fixed on to the ceiling and the floor of the test section. The gaps between the dummies and each end of the model were approximately 0.5mm to 1.0mm wide and covered with very flexible thin rubber to contraception use. The cylinder of each diameter was pulled to the walls by means of three 0.5mm diameter wires to stop vibration due to Kármán vortex. Calibration of the balance with wind off and tare measurement were made in a usual manner in tunnel practice.

A 32mm cylinder mounted on the balance is shown in Fig. 10. Drag coefficient of a 100mm disc was determined also on the balance. The disc is 99.9mm in diameter, 0.3mm thick at the edge where it has the angle of 7.19 degrees, made of a steel plate and buff-finished to mirror-like surface.

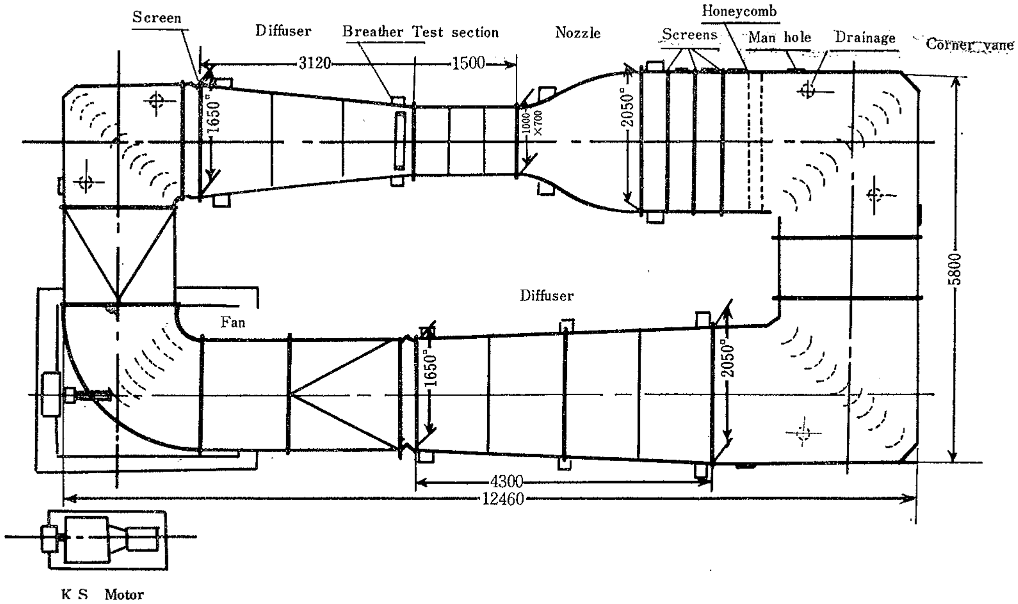

Fig. 1. Plan view of the 1.0×0.7 m low speed wind tunnel of Tottori university

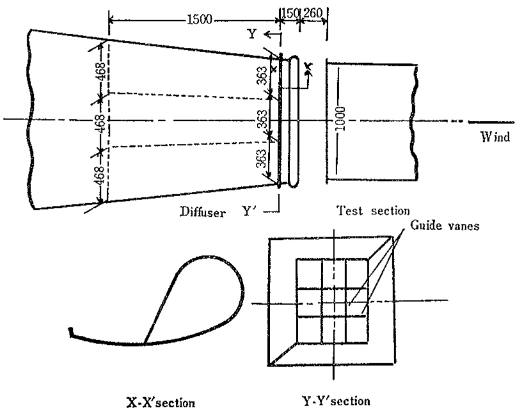

Fig. 2. Diffuser after improvement

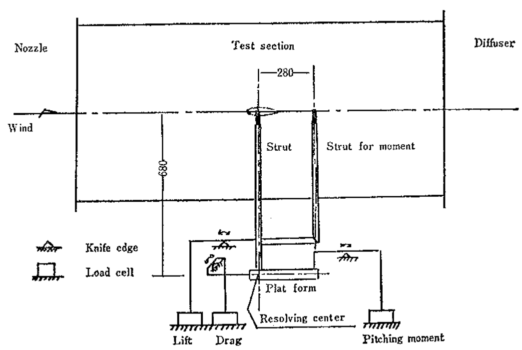

Fig. 3. Balance skeleton

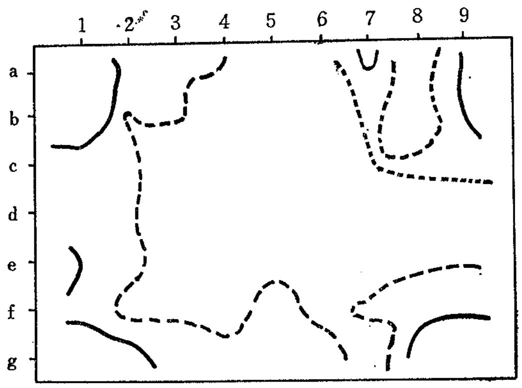

Fig. 4. Equi-velocity lines at 52m/s in the inlet-plane seen from downstream

------ $(c/c_o-1)\times100=0.5\%$

——— 〃 $=1.0\%$

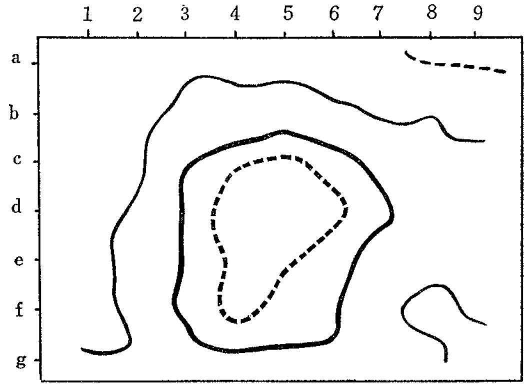

Fig. 5. Equi-velocity lines at 52m/s in the outlet-plane seen from downstream

.... $(c/c_o-1)\times100=0.5\%$

——— $=1.0\%$

——— $=2.0\%$

------- $=3.0\%$

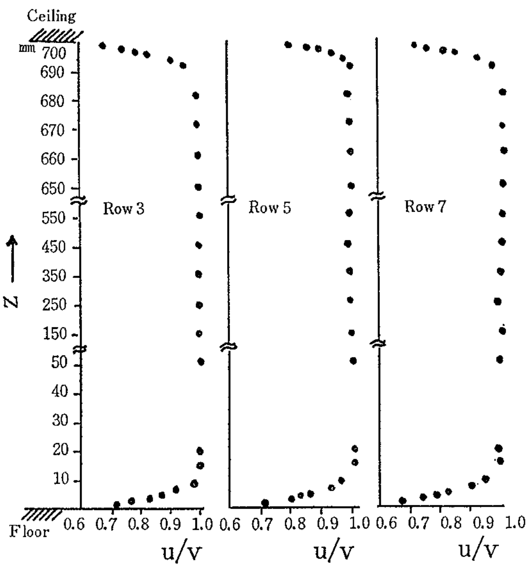

Fig. 6. Velocity profiles at rows 3,5and 7 of the inlet-plan u/v : local to center velocity ratio

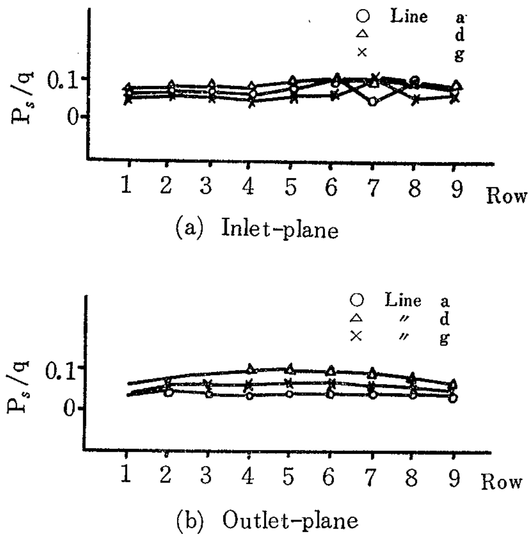

Fig. 7. Static pressure distributions at the inlet-and ontlet-planes

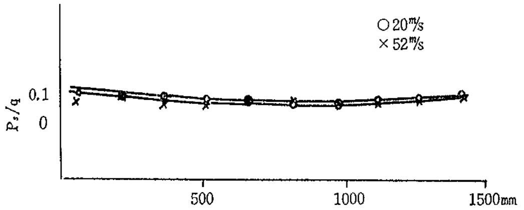

Fig. 8. Longitudinal static pressuse distribution

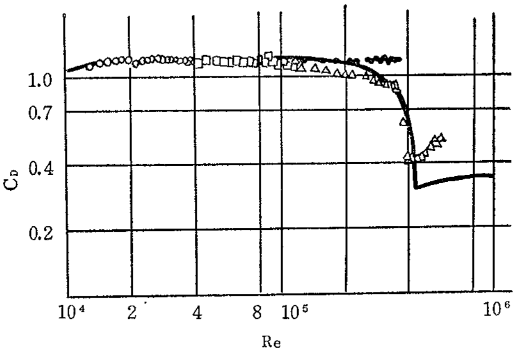

Fig. 9. Drag coefficients of two dimensional circular cylinders and a disc
• : disc, other symbols : cylinders